

# Semi-Automatic Pallet Pick-up as an Advanced Driver Assistance System for Forklifts

Benjamin Molter, Johannes Fottner  
Chair for Materials Handling, Material Flow, Logistics  
Technical University of Munich, Germany  
{benjamin.molter, j.fottner}@tum.de

**Abstract**—This paper presents a novel advanced driver assistance system for human-operated forklifts in logistical scenarios. The system helps the operator to pick up wooden pallets by performing a collision-free insertion of the forks into the pallet. For this purpose, the assistance system takes over the steering function of the vehicle while it approaches the pallet. A 3D camera-based system is used to detect and localize the pallets while driving. For every localized pallet, a trajectory is calculated which has to fulfill certain conditions. These include an at least curvature continuous course and limiting vehicle parameters, such as a limited steering angle. Furthermore, the necessary user interface for the correct selection of the target pallet and the activation of the assistance function is presented. Finally, a technical method is described to realize the steering intervention on an existing forklift.

**Keywords**—*advanced driver assistance system, forklift, pallet pick-up, object detection, trajectory calculation*

## I. INTRODUCTION

Advanced driver assistance systems are becoming increasingly important for different types of vehicles. Pioneers in this discipline are automobile manufacturers. With each new generation of cars, new or improved advanced driver assistance systems are presented. For industrial trucks, such as counterbalance forklifts, only a few specific versions of such systems are available. The long-term goal of the automotive industry is autonomous driving on public roads. Modern advanced driver assistance systems for cars pave the way for this goal by making partial functions, such as lane guidance, possible. The manufacturers of industrial trucks, or in particular the manufacturers of automated guided vehicles, have been offering autonomous vehicles for in-house material transport purposes since the 1960s [1]. Therefore, their goal for human-operated forklifts is not the replacement of the driver, but assistance in the task of vehicle operation.

The typical forklift operation consists of the pick-up and drop-off of cargo. In most cases, the load is on load carriers, which have openings for the forks of the forklift. The most well-known load carriers are pallets made of wood or plastic as well as metal pallet cages. The insertion of the forks into the openings of the pallet requires skill and experience on the part of the operator due to the small spatial conditions in warehouses. The forklift driver must align the forks as accurately as possible for insertion into the corresponding openings of the pallet.

Often there is a great deal of time pressure in the

operative business due to the large number of transport orders. In particular, inexperienced drivers, such as novice drivers or temporary workers, can cause minor accidents under these circumstances [2]. For novice drivers, on the one hand the unusual rear wheel steering and, on the other hand, the more or less simultaneous operation of the lifting device is challenging. Temporary workers have to cope with forklifts from multiple manufacturers with different types of controls. Careless operation of the forklift can damage the load or the load carriers with the forks. In the worst-case scenario, the pallet is on a warehouse rack and is pushed down from its cross beams. In addition to the impact on personal safety, such incidents also cause economic material damage. Against this background, we present our research and introduce a novel driver assistance system, that assists the operator of a forklift in the process of pallet pick-up.

## II. RELATED WORK

Basically, assistance systems for forklifts can be divided into two categories: safety systems and assistance systems [3]. The first ones are required for the safe operation of the forklift and must comply with the applicable standards and laws. The reliability of such systems must be proven. Assistance systems, on the other hand, aim to make operation of the vehicle more ergonomic and efficient.

In the field of advanced driver assistance systems for forklifts, so far only a few scientific researches have been presented. The work of Kleinert and Overmeyer [4] presents a system that visually supports the driver using a collision indicator with traffic light colors when he is inserting the forks into the pallet. They have integrated a 3D camera, which works according to the time-of-flight principle, into the tip of one fork. For this reason, the assistance function can only be performed if the forks point in the direction of the target pallet. In general, the driver gets only a hint for further operation. The system does not intervene in vehicle control.

Other work has been presented in the context of avoiding collisions with other pedestrian workers around forklifts. Lang and Günthner [5], for example, show a collision warning system for forklifts. A rear-facing combined 2D and 3D camera captures the environment. Depending on the movements detected, targeted warnings are issued in the event of imminent collisions with people. There are no warnings about collisions with logistical infrastructure. Awolusi et al. [6] introduce another system for the same purpose based on magnetic field proximity-sensing. The forklift and the pedestrian workers are equipped with

appropriate devices. As the two devices approach each other, the smaller unit, worn on the body of the worker, affects the magnetic field of the unit on the forklift. The small unit warns the wearer by means of vibration and an audible signal. There is also no intervention in the vehicle control. Zimmert and Sawodny [7] present in their work an active damping control for the lift mast of reach trucks. In particular, shifting the mast forward at high lifting heights and with heavy cargo creates oscillations that prevent rapid work. Safe storage in pallet racks is only possible if the mast and thus also the cargo no longer oscillates. The control algorithm was implemented on the control unit of the reach truck, so that an intervention in vehicle control could be realized.

The manufacturers of industrial trucks already offer some driver assistance systems as equipment options. For these systems, however, there is no scientific consideration. In addition, the supplier industry also offers various retrofit products. The focus of these products is on the detection of collisions with the infrastructure or pedestrian workers, simple visual assistance by 2D video cameras or location-dependent restrictions on vehicle speed or lift height.

### III. SYSTEM OVERVIEW

The advanced driver assistance system presented here supports the operator of a forklift during the pallet pick-up process. The system takes over the steering function and thus enables a collision-free insertion of the forks in the corresponding openings of the pallet. The accelerator and brake pedal remain under the control of the operator. Therefore we call our system semi-automatic. For this first version of the assistance system, we focus on standardized euro pallets [8] that are directly located on the ground.

In Fig. 1, the procedure of the assistance function is described in a series of diagrams: Starting from a transport order with a source and a sink, the operator drives the forklift to the position where the load is located. A 3D camera, mounted on the forklift and oriented in the direction of movement, continuously records the environment. With methods of computer vision, the depth images of the 3D camera are searched for pallets. Upon successful detection and localization, a valid drive trajectory for a collision-free pick-up is calculated for each pallet. The pallets for which a

trajectory could be calculated are displayed to the operator on a screen. After selecting the target pallet, the assistance system takes over the steering function. The operator operates the accelerator and the forklift follows the calculated trajectory. By doing this, the detection and localization of the pallet is continuously being performed to get an updated relative position with respect to the forklift. This is necessary for the control loop of the steering angle. The operator is responsible for the driving speed. He must always observe the entire environment when executing the system and brake the vehicle in the event of an emergency. In addition, it is always possible to override the assistance function by manual steering.

The forklift follows the trajectory until it is optimally aligned straight in front of the pallet. Further steering movements are no longer required for the pallet pick-up process. An ultrasonic distance sensor records the distance between the fork carriage and the pallet. Driving straight ahead moves the forks under the pallet until the distance sensor detects that the fork carriage is approaching the pallet. The operator receives a corresponding note on the screen. The assistance function has finished. The operator again has complete control over all functions of the forklift and can continue the transport to the destination to fulfill the transport order.

In the following subsections, the three main components (these are marked with an \* in Fig. 1) of the system are explained in detail according to their function. On the one hand the occurring challenges are described and on the other hand the found solutions are presented.

#### A. Pallet Detection and Localization

We use a Microsoft Kinect v2 camera to detect and locate pallets. This provides both a 2D color image and a 2D grayscale depth image based on the time-of-flight principle. The color image is not used in our approach. The depth image is converted into a 3D point cloud data format on the connected computer. The point cloud allows a direct reading of Cartesian coordinates in relation to the camera. The static camera position on the top of the back of the forks is taken into account by an offset.

We use our self-developed pallet detection and localization algorithm [9]. It uses the known geometric properties of the pallet components as a basis for detection and works without

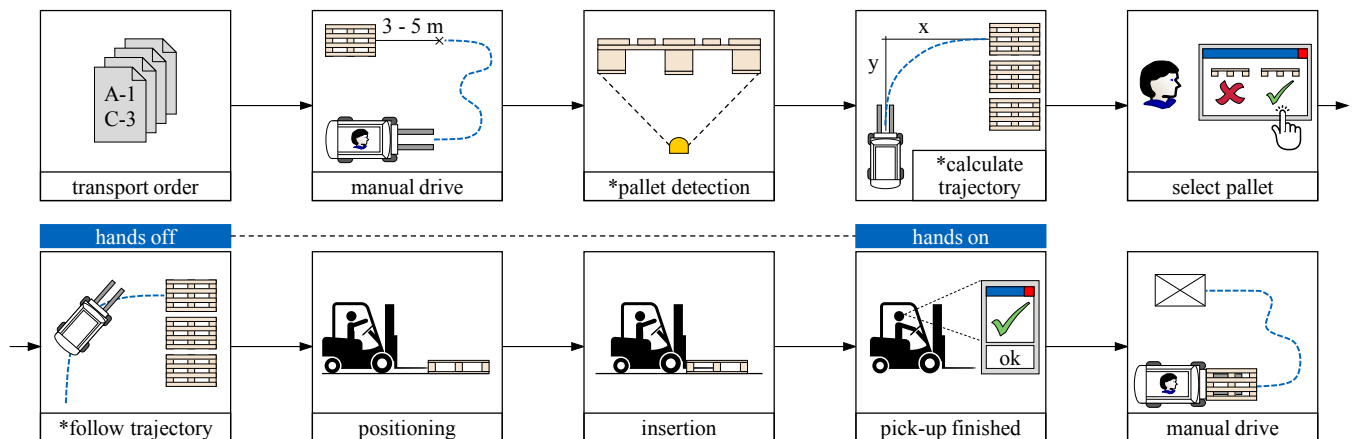


Fig. 1. Schematic representation of the semi-automatic pallet pick-up as an advanced driver assistance system. Diagrams marked with an asterisk are explained in the subsections of section III.

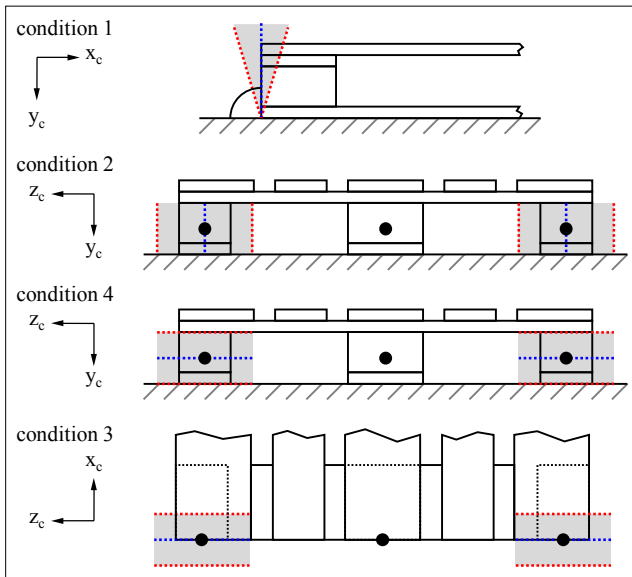


Fig. 2. All four geometrical conditions for pallet detection, when the pallet has an orientation of  $90^\circ$  to the Kinect camera. Gray areas indicate the range of valid values. Black points represent centroids.

any a priori information or artificial markers. Our algorithm is based on finding vertical surfaces with respect to the ground plane in the point cloud, which represent the three wooden blocks of a euro pallet. Four kinds of geometrical checks set up our detection pipeline, where no artificial markers on the pallets are needed (Fig. 2). Processing the recorded point cloud starts with the region growing algorithm, which is implemented in the Point Cloud Library, an open-source library for the processing of point clouds. For each surface found, the centroid and the normal vector are calculated. The normal vector is used to check whether the segmented area is vertical or not. Due to sensor-induced noise even slightly inclined surfaces are considered further. The distances of the wooden blocks are fixed according to the uniform dimensions of a euro pallet. By checking the Euclidean distance between the centroids, pairs can be found which correspond to the characteristic wooden blocks of a pallet. Once the three wooden blocks have been found, the relative position and orientation is determined using the calculated centroids.

The challenge here lies in detecting pallets, which are orientated up to  $90^\circ$  in relation to the sensor plane. This scenario is very common whenever a forklift drives through an aisle in a pallet rack storage with pallets to the left and right. To use the assistance function, the identification and localization of pallets must be carried out while driving. Therefore, the processing of the point clouds must be done within a set time limit.

### B. Trajectory Calculation

Generally speaking, a forklift is a non-holonomic system, which has a limited number of possible directions of movement. Assuming that there is no lateral sliding of the tires, the velocity vector in the center of an unsteered axle is always parallel to the vehicle's longitudinal axis. The velocity vector in the middle of a steered axle rotates equally with the steering angle, which is mechanically limited to a maximum deflection. Accordingly, non-holonomic vehicles

can only follow tangent-continuous paths whose curve radii are greater than or equal to a minimum radius over the entire length.

Counterbalance forklifts are available as three-wheel and four-wheel versions. They differ by the maximum possible steering angle. In the case of the four-wheel forklift truck, the smallest curve radius corresponds to the smallest pivot point distance. The pivot point distance for a three-wheel forklift is 0. For this reason, it can turn around the center of its front axle at full steering angle on the spot.

A curve that is continuous in its angular course, but not continuous in its curvature course, is called a  $G^1$  continuous curve (geometrically continuous of first order). Consequently, the non-holonomic vehicle must stop at non-continuous curvature points and change its steering angle at standstill to follow the next curve section. Since this is not suitable for practice, there is a minimum requirement that the trajectory must have a continuous course of curvature ( $G^2$ ). In particular, the connection of different geometric segments requires a transition element to meet this requirement. Fig. 3 shows a simplified example: Although the transition from a straight line to a circular arc is continuous, the curvature  $\kappa$  at the transition point is discontinuous. By inserting an Euler spiral (clothoid) as a transition element, the jump of the curvature  $\kappa$  can be prevented. The curvature of the Euler spiral is proportional to its arc length.

In addition to these requirements, two additional mathematical constraints can be formulated which increase the quality of the trajectory. In the next higher geometric continuity of order three ( $G^3$ ), besides the curvature, the curvature change is also continuous. This reduces lateral slipping over the tire contact area compared to a  $G^2$  curve, because the steering movements are no longer jerky, but the steering speed is uniformly accelerated and decelerated without any jumps. Furthermore, the lowest possible change in the steering angle relative to the arc length can be seen from the aspect of safety. For example, if the lateral acceleration of the forklift when cornering is a design criterion for safety against overturning, the vehicle speed must be reduced with narrowing curves, so as not to exceed a maximum lateral acceleration.

Here there is a conflict of objectives: On the one hand, the forklift should arrive at the destination pallet as quickly as possible when processing a transport order. According to Dubins [10], the shortest, drivable path for a non-holonomic vehicle is achieved by circular arcs with the smallest possible radii. On the other hand, strong curvature changes and associated speed changes should be avoided. In addition to the aforementioned Euler spiral, there are other mathematical approaches for calculating trajectories.

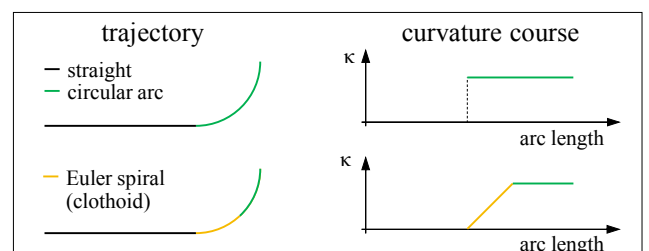


Fig. 3. Schematic examples of  $G^1$ - and  $G^2$ -trajectories (left) and their associated curvature courses (right).

The Fermat spiral is an Archimedean spiral with the winding factor  $n=2$ . It is therefore relevant for the generation of trajectories because it has a continuous curvature beginning at zero and can thus connect a straight line  $G^2$ -continuous with a circular arc.

Bézier curves are mainly used to create free-form curves and surfaces. They are calculated using the De-Casteljau's algorithm, which interpolates repeatedly linearly between points. The shape of a Bézier curve is determined by the number and location of its control points. It runs tangentially through the starting point and end point of the polygon course.

Another path planning approach works by means of  $\eta$ -splines and was presented by Piazzini et al. [11]. Two points in the plane are connected by a polynomial function. Depending on the degree of the polynomial, not only the tangent angles but also the curvatures and their derivatives at the start and end points can be specified. Additional  $\eta$ -parameters can be used to influence the derivation functions of the spline and thus its shape. In general, the exponent of an  $\eta$ -spline corresponds to geometric continuity. The  $\eta^3$ -spline considered here therefore is  $G^3$  continuous and is described by a polynomial function of degree 7.

Table I gives an overview of possible approaches for trajectory calculation. In addition to geometric continuity, an assessment is made as to whether the respective approach can take into account a limitation of the steering angle (four-wheel vehicle). It also indicates how well the trajectory can be controlled in its course and how flexible it is.

The advantage of the  $\eta$ -splines over the clothoid and the Archimedean spiral is their high flexibility. Any number of states can be specified at the start and end points, and an infinite number of trajectories can be generated under these circumstances. At the same time, the low computational complexity of the polynomials is very well suited to the objective of real-time capability in practical use. We therefore choose the  $\eta^3$ -spline from [11] as the basis for our trajectory calculation.

The input parameters for calculating a trajectory can be divided into location and vehicle information. The localization provides the relative distance  $(x_0, y_0)$  and orientation  $\theta_0$  of the pallet to a fixed reference point on the forklift. Together with the current steering angle  $\delta_0$  and the steering angle speed  $\dot{\delta}_0$ , this information gives the definition for the starting point  $\mathbf{p}_0$  of the trajectory.

TABLE I. OVERVIEW OF MATHEMATICAL APPROACHES FOR PATH PLANNING

	continuity	steering limit	course	flexibility
straight	$G^0$	$= 0$	controlled	low
arc	$G^1$	yes	controlled	low
Euler spiral	max. $G^2$	yes	controlled	low
Fermat's spiral	max. $G^2$	yes	controlled	low
Bézier curve	dependent from number of control points	no	controlled	high
$\eta$ -spline	$\eta^n \rightarrow G^n$	no	conditional controlled	high

Instead of the steering angle, the curvature  $\kappa_0$  is used as the reciprocal of the radius and its time derivative  $\dot{\kappa}_0$  for the trajectory description. The scenario is shown from the top view for a single pallet in Fig. 4. The objective is to model the trajectory in a stationary coordinate system, which has its origin in the middle of the of the pallet. This corresponds to the idea that the forklift moves towards the pallet and not vice versa. However, a world-wide coordinate system is not provided because the driver assistance system is not globally oriented. At the end point  $\mathbf{p}_1$  of the trajectory, the forklift is centered in front of the pallet. The steering angle  $\delta_1$  is  $0^\circ$ , so that the assistance system can drive the forks under the pallet without any further steering movement.

According to (1) and (2), for the mathematical description of a polynomial function of degree 7, a total number of 16 coefficients ( $\alpha_0 - \alpha_7$  and  $\beta_0 - \beta_7$ ) must be defined.

$$x(u) = \alpha_0 + \alpha_1 u + \alpha_2 u^2 + \alpha_3 u^3 + \alpha_4 u^4 + \alpha_5 u^5 + \alpha_6 u^6 + \alpha_7 u^7 \text{ with } u \in [0, 1] \quad (1)$$

$$y(u) = \beta_0 + \beta_1 u + \beta_2 u^2 + \beta_3 u^3 + \beta_4 u^4 + \beta_5 u^5 + \beta_6 u^6 + \beta_7 u^7 \text{ with } u \in [0, 1] \quad (2)$$

10 of the 16 unknowns are defined by specifying the states at the starting point  $(x_0, y_0, \theta_0, \kappa_0, \dot{\kappa}_0)$  and at the end point  $(x_1, y_1, \theta_1, \kappa_1, \dot{\kappa}_1)$ . The remaining 6 degrees of freedom are then determined via  $\eta$ -parameters, which are defined as follows [12]:

$$\eta_1 := \sqrt{x_0'^2 + y_0'^2} \quad (3)$$

$$\eta_2 := \sqrt{x_1'^2 + y_1'^2} \quad (4)$$

$$\eta_3 := x_0'' \cos \theta_0 + y_0'' \sin \theta_0 \quad (5)$$

$$\eta_4 := x_1'' \cos \theta_1 + y_1'' \sin \theta_1 \quad (6)$$

$$\eta_5 := x_0''' \cos \theta_0 + y_0''' \sin \theta_0 \quad (7)$$

$$\eta_6 := x_1''' \cos \theta_1 + y_1''' \sin \theta_1 \quad (8)$$

The terms  $\eta_1$  (3) and  $\eta_2$  (4) are referred to as "parametric speed".  $\eta_3$  (5) and  $\eta_4$  (6) then assume the meaning of an acceleration, and  $\eta_5$  (7) and  $\eta_6$  (8) the meaning of an acceleration change. The odd indexes refer to the starting point and the even indices to the end point.

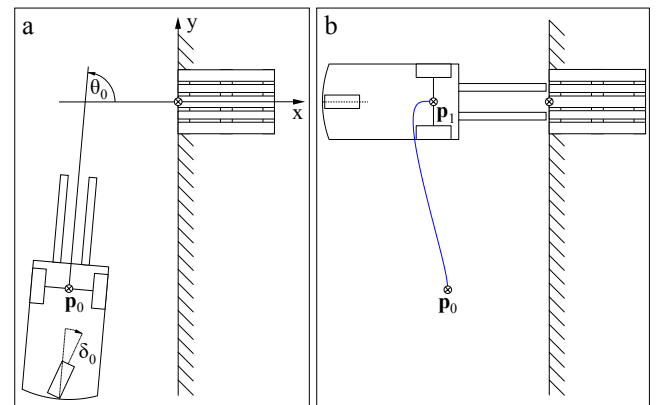


Fig. 4. a) Forklift position and orientation at the start point  $\mathbf{p}_0$  and b) at the end point  $\mathbf{p}_1$  of the trajectory (blue line). The trajectory is an  $\eta^3$ -spline and shows the course of the vehicle pivot point.

The 16 coefficients  $\alpha_i$  and  $\beta_i$  of the now completely determined  $\eta^3$ -spline are calculated using equations from [12]. The  $\eta$ -parameters can be chosen freely and thus influence the shape of the trajectory. The defined conditions for the starting point and end point are thereby not violated.

### C. Assistance Function

After the localization of pallets and the calculation of trajectories, the real phase of the assistance system for the operator of the forklift begins. The 2D color image of the Kinect camera is displayed on a touchscreen in the driver's cab. Palettes for which a valid trajectory has been calculated are marked with a clearly visible, colored frame. For further consideration, it can be assumed that the pallet belonging to the current transport order has been selected by the operator. The assistance system then takes over the steering function of the forklift. The operator controls the accelerator pedal until the forks are moved completely under the pallet. At the same time, the operator has the task of monitoring the environment in order to recognize critical and life-endangering situations at all times. In such situations, the system recognizes that the driver wants to override the assistance system by quick and jerky steering wheel movements or by operating the brake pedal. This eliminates the need for safety sensors according to performance level d (EN ISO 13849) and SIL 2 (IEC 61508).

An important aspect of driver assistance systems is their acceptance by the user. In combination with a positive user experience, the use of the system can be favored. For this reason, the state of the driver assistance system for the operator must be clearly visible at all times, particular since responsibility for one of the main functions of the vehicle, steering, alternates between the system and the operator. On the existing monitor important information is visualized by pictograms and text. A colored border of the whole screen content indicates the state of the system. If the system is ready to take over the steering by selecting a pallet, then this border is green. While the system steers automatically, it changes to orange. The frames of recognized palettes are then no longer displayed.

## IV. TESTS AND RESULTS

### A. Pallet Detection and Localization

We first tested the detection and localization of pallets in a static scenario where the forklift was at a standstill. This was followed by a dynamic test in which the vehicle approached a pallet at low speed  $< 1$  m/s. For both scenarios, the true-positive localizations and the calculation rate were evaluated. Due to the elaborate processing of 3D data, the algorithm in this first version provides the relative pose of the detected palettes at least every 66.6 ms (15 fps) in the dynamic scenario. A detailed evaluation can be found in [9]. In Fig. 5 the detection pipeline is shown with recorded point clouds. The first point cloud a) shows the 90° scenario for a single pallet. The ground plane found is colored blue. In the front area the forks are visible. The second point cloud b) is cropped down to the pallet. It shows the results of the detection steps: Every vertical plane found is visualized. The colorization is random and just for better visualization. Black points do not belong to any segments.

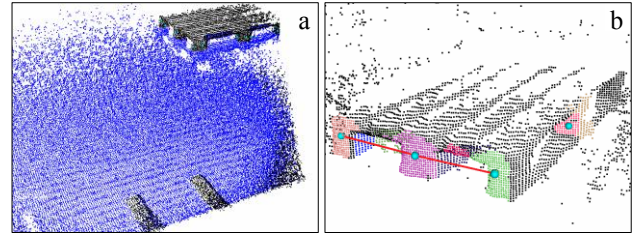


Fig. 5. a) Point cloud of the 90° scenario with detected ground plane (blue) and b) point cloud segmentation of vertical planes with region growing algorithm and visualization of the geometrical pallet detection (red line).

The computed centroids are visualized as small light blue spheres on the planes found. Between the centroids a red line is drawn, that shows a valid pallet by the geometrical pallet detection. The determined relative positions and orientations of the found pallets are transmitted to the next subsystem.

### B. Trajectory Calculation

For the selected  $\eta^3$ -spline, a MATLAB software tool was programmed to test the mathematical properties in a simulation. The tool visualizes the calculated trajectory in the form of a top view (see blue line in Fig. 4) and also shows the courses of the forklift orientation  $\theta$ , the curvature  $\kappa$  and the steering angle  $\delta$  and its time derivatives  $\dot{\kappa}$  and  $\dot{\delta}$ . In Fig. 6, the courses of these values are plotted along the trajectory length  $s$ , which reaches the target position  $\mathbf{p}_1$  in front of the pallet at 4.32 m.

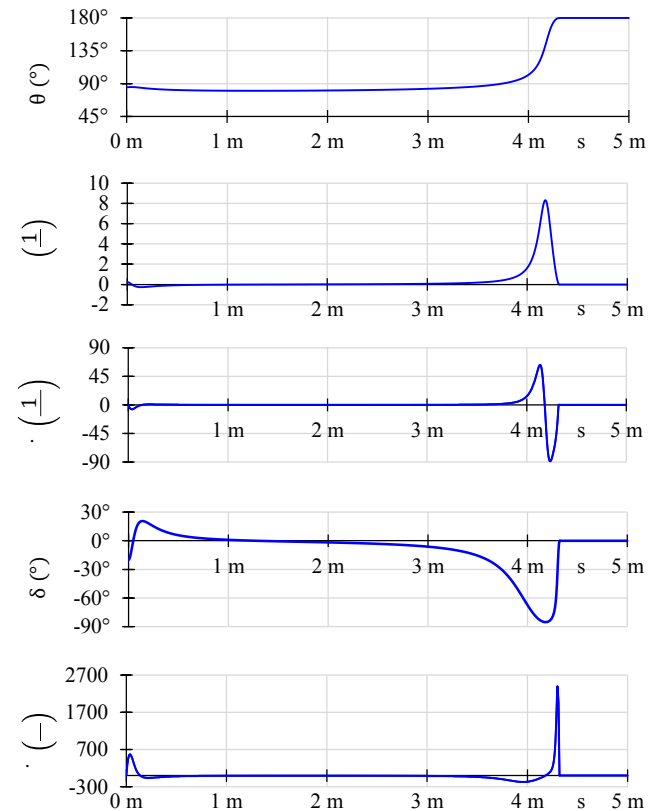


Fig. 6. Course of the curves plotted over the trajectory length  $s$ : angle alignment  $\theta$  between forklift and pallet, curvature  $\kappa$  and curvature change  $\dot{\kappa}$  as well as the steering angle  $\delta$  of the forklift and its derivation  $\dot{\delta}$ .



The starting values for the calculation have been selected as examples:  $x_0 = -1.7$  m,  $y_0 = -4.0$  m,  $\theta_0 = 85^\circ$ ,  $\delta_0 = -20^\circ$  ( $\kappa_0 = 0.248$  1/m),  $\dot{\delta}_0 = 0$  °/m ( $\dot{\kappa}_0 = 0$  1/m<sup>2</sup>). It can be seen that both the curvature  $\kappa$  and even the curvature change  $\dot{\kappa}$  are continuous over the entire length of the trajectory. The steering angle  $\delta$  reaches its maximum value shortly before reaching the end point. The limit of  $90^\circ$  is not violated. The following  $\eta$ -parameters were calculated for the selected start pose:  $\eta_i$  ( $i = 1 \dots 6$ ) =  $\{2, 1, 20, -1, 0, 0\}$ .

In [13]  $\eta_1 = \eta_2 = \|\mathbf{p}_1 - \mathbf{p}_0\|$  is proposed. These values lead to large values of the curvature in the end point  $\mathbf{p}_1$  of the trajectory. By including the curvature, this problem has been addressed in (9) and (10).

$$\eta_1 = \frac{\|\mathbf{p}_1 - \mathbf{p}_0\|}{1 + |\kappa_0|} \quad (9)$$

$$\eta_2 = \frac{\|\mathbf{p}_1 - \mathbf{p}_0\|}{1 + |\kappa_1|} \quad (10)$$

The nonlinear dependencies make it difficult to identify optimal  $\eta_3$ - and  $\eta_4$ -parameters, so that only by means of an iterative approach can a conditionally optimal solution be found. With the simulation, a parameter study was carried out to obtain a range of valid  $\eta$ -parameters for as many initial positions as possible. The following value ranges were determined for 525 different, realistic starting poses:  $\eta_3 = 0 \dots 30$  and  $\eta_4 = -22.75 \dots 0$ .  $\eta_5 = \eta_6 = 0$ , because no acceleration change is taken into account here.

### C. Vehicle Interface

We use a Jungheinrich EFG 220 three-wheel forklift for our tests. The steering function of this vehicle is designed as steer-by-wire. Our intervention in the steering signal is between the rotary encoder on the steering wheel and the steering control unit (Fig. 7). The encoder provides a sin/cos signal in the range 0.5...4.5 V. We use a PLC with analog inputs and outputs to get the current steering wheel position and to pass on our calculated steering angle to the control unit. Since the desired steering angle changes with the course of the trajectory, a check of the current angle of the rear wheel is necessary to implement a control loop. The angle of the rear wheel is provided as a message via the vehicle's own network (CAN). The PLC is also responsible for switching between normal driving (signal loop through) and assistance mode.

## V. CONCLUSION AND OUTLOOK

This paper presents a new driver assistance system for human-operated forklifts. In a logistical scenario, the system enables collision-free insertion of the forks into a pallet. For this, the operator hands over the steering function to the assistance system. Using a 3D camera pallets are detected and localized, which are located in front of the forklift in the field of view of the camera. For each localized pallet a curvature continuous trajectory is calculated. We use a so called  $\eta^3$ -spline, which is based on a polynomial function of degree 7. The operator selects the desired palette on a screen and then controls only the accelerator and brake pedal.

The results show, that the driver assistance system can localize pallets in common logistical scenarios at low speeds  $< 1$  m/s. Furthermore, it is shown that the selected  $\eta^3$ -splines

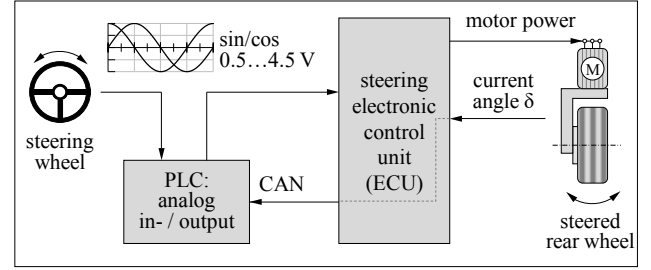


Fig. 7. Schematic of the implemented steering intervention with a PLC via the analog voltage signal of the rotary encoder of the steering wheel.

are suitable for calculating valid trajectories with respect to continuous curvature and limiting vehicle parameters.

Future work will be the improvement of our pallet detection for higher velocities. Also, the human machine interface must be examined to allow a smooth, economical assistance function, which will be accepted by the forklift operators. In addition, field tests must be performed to evaluate that the proposed assistance system enables faster and safer work.

## REFERENCES

- [1] VDI 2510, Association of German Engineers – VDI Society Production and Logistics, "Automated Guided Vehicle Systems (AGVS)", 2005.
- [2] DC Velocity (2013, Mar.), "Material Handling – How to reduce pallet damage". [Online] Available: [www.develocity.com/articles/20130318-how-to-reduce-pallet-damage](http://www.develocity.com/articles/20130318-how-to-reduce-pallet-damage). Accessed on: Feb. 26 2018.
- [3] German Engineering Federation (VDMA) – Materials Handling and Intralogistics (2016, May.), "Position paper assistance systems on industrial trucks [Original title: Positionspapier Assistenzsysteme an Flurförderzeugen]". [Online] Available: <http://foerd.vdma.org/viewer/-/v2article/render/22409378>. Accessed on: Feb. 27 2018.
- [4] S. Kleinert and L. Overmeyer, "Integration of 3D Camera Systems on Forklift Trucks [Original title: Integration von 3D-Kamerasystemen am Gabelstapler]," *Scientific Society for Technical Logistics (WGTL): Logistics Journal*, vol. 2013, no. 10, 2013.
- [5] A. Lang and W. A. Günthner, "Evaluation of the Usage of Support Vector Machines for People Detection for a Collision Warning System on a Forklift," *HCI in Business, Government and Organizations. Interacting with Information Systems (HCIIBGO)*, pp. 322–337, 2017.
- [6] I. Awolusi, S. Song, and E. Marks, "Forklift Safety: Sensing the Dangers With Technology," *The American Society of Safety Engineers: Professional Safety*, vol. 62, no. 10, pp. 36–39, 2017.
- [7] N. Zimmert and O. Sawodny, "Active damping control for bending oscillations of a forklift mast using flatness based techniques," *Proceedings of the American Control Conference (ACC)*, pp. 1538–1543, 2010.
- [8] EN 13698-1:2003, European Committee for Standardization, "Pallet production specification Part 1: Construction specification for 800 mm x 1200 mm flat wooden pallets", 2003.
- [9] B. Molter and J. Fottner, "Real-time Pallet Localization with 3D Camera Technology for Forklifts in Logistic Environments," *unpublished, submitted to IEEE International Conference on Service Operations and Logistics, and Informatics (SOLI)*, 2018.
- [10] L. E. Dubins, "On Curves of Minimal Length with a Constraint on Average Curvature, and with Prescribed Initial and Terminal Positions and Tangents," *American Journal of Mathematics*, vol. 79, no. 3, pp. 497–516, 1957.
- [11] A. Piazzzi, M. Romano, and C. G. L. Bianco, "G<sup>3</sup>-splines for the path planning of wheeled mobile robots," *European Control Conference (ECC)*, pp. 1845–1850, 2003.
- [12] A. Piazzzi, C. G. Lo Bianco, and M. Romano, "Smooth Path Generation for Wheeled Mobile Robots Using  $\eta^3$ -Splines," in *Motion Control*, F. Casolo, Ed.: InTech, 2010.
- [13] A. Piazzzi, C. G. Lo Bianco, M. Bertozzi, A. Fascioli, and A. Broggi, "Quintic G<sup>2</sup>-splines for the iterative steering of vision-based autonomous vehicles," *IEEE Transactions on Intelligent Transportation Systems*, vol. 3, issue 1, pp. 27–36, 2002.